

Resonance in the Dirac Harmonic Oscillator

Harold V. McIntosh

Departamento de Aplicación de Microcomputadoras
Instituto de Ciencias, Universidad Autónoma de Puebla
Apartado Postal 461, (72000) Puebla, Puebla, México.

November 24, 2000

Abstract

Detailed examination of the resonances in the Dirac harmonic oscillator, using results from the differential equation solver SERO.

Contents

1	The Dirac equation	2
2	Matrix differential equations	2
3	Numerical integration with graphical presentation	4
4	Zero mass and its subsequent enhancement	5
5	The Weyl-Titchmarsh m-function	8
6	Dependence of spectral density on mass	14

1 The Dirac equation

Soon after Dirac published his relativistic wave equation [1] in 1928, it was tried out with a variety of potentials, from which a gradual awareness of some of its strange properties arose. From the beginning, of course, it was evident that solutions with arbitrarily negative energies could exist, but as time went on, it was found that they could not always be cleanly separated from the positive energy solutions.

Even so, the harmonic oscillator never seems to have been a specific object of study. It was one of the cases included in a systematic review of power law potentials, mostly negative powers, which might induce singularities at the origin of the second order differential equation which one wanted to quantize.

Nikolsky [3] examined it in 1930, Postepska [4] five years later, after which it seems to have laid dormant until Sewell's perturbation approach [5] in 1949. The latter immediately attracted Titchmarsh's attention [6] because the spectrum was actually a continuum with sharp resonances amenable to his general theory of eigenfunction expansions based on the m -function of Weyl's thesis [2].

In recent years another differential equation has come to be called the "Dirac harmonic oscillator," with applications to quark physics. What has happened is that Dirac's version of a relativistic wave equation does not exhaust all the possibilities for simple multicomponent wave equations.

In one dimension, there are four linearly independent 2×2 matrices which are usefully referred to a quaternion basis. To keep real matrices, a somewhat Lorentzian version of the quaternions is required wherein the squares of two of them are $+1$ while only the third is -1 ; all of Hamilton's quaternions square to -1 .

Whatever the preferred symbolism, both the Schrödinger equation and the Dirac equation have coefficient matrices which are linear combinations of \mathbf{i} and \mathbf{j} . There is no reason to omit \mathbf{k} from the construction of the coefficient matrix; indeed such a term would arise from separating Dirac's equation had an angular momentum term been present.

From the point of view of symmetry and accidental degeneracy, the new variant not only has a discrete spectrum, but an interesting symmetry group. It also reflects properties ascribed to the quark model of nuclear matter, so it is hardly surprising that it has become an object of study in its own right. Nevertheless, the present discussion is primarily concerned with resonance and continuum wave functions, so it is confined to the "classical" Dirac Harmonic Oscillator.

Most of the figures included in this report were obtained with the CalComp plotter attached to the PDP-10 computer at the Instituto Nacional de Energía Nuclear in Salazar, using a program collection called **SERO** together with the graphics package **<PLOT>**. In the interim these programs have been adapted to a series of microcomputers, and to the types of visual display which they employ; some of them have also been used.

2 Matrix differential equations

All in all, the Dirac harmonic oscillator is a good place to study resonances, especially if much smaller masses are considered than the ones which characterize the actual experience of physicists. Of course, that makes a comparison with experiment correspondingly difficult.

The one-dimensional Dirac equation for a particle of rest mass m_0 has a matrix form

$$\frac{d\mathbf{Z}(x)}{dx} = \begin{pmatrix} 0 & m_0 + (V(x) - E) \\ m_0 - (V(x) - E) & 0 \end{pmatrix} \mathbf{Z}(x). \quad (1)$$

The substitutions

$$k = [(V - E)^2 - m_0^2]^{1/2}, \quad \sigma = \left(\frac{V - E + m_0}{V - E - m_0} \right)^{1/2}$$

lead to a convenient solution matrix,

$$\mathbf{Z}(x) = \begin{pmatrix} \cos k x & \sigma \sin k x \\ (1/\sigma) \sin k x & \cos k x \end{pmatrix}, \quad (2)$$

but only for a constant energy difference $E - V$, and for real k . Formally the result holds for imaginary k but in that case, a classically forbidden region, it is preferable to redefine both k and σ to make them real and then use hyperbolic functions.

There are other approximations which are useful; for example when the mass is small enough to be neglected, the coefficient matrix is antisymmetric. Setting

$$\varphi(x, x_0) = \int_{x_0}^x (v(t) - E) dt \quad (3)$$

the solution becomes

$$\mathbf{Z}(x) = \begin{pmatrix} \cos \varphi(x, x_0) & -\sin \varphi(x, x_0) \\ \sin \varphi(x, x_0) & \cos \varphi(x, x_0) \end{pmatrix} \mathbf{Z}(x_0), \quad (4)$$

which is a pure rotation in the phase plane.

There is a standard procedure for correcting an approximate coefficient matrix in a system of differential equations. Suppose that the full coefficient M is split into a sum

$$M = A + B, \quad (5)$$

wherein A is the convenient approximation and B is a correction, not necessarily small. All kinds of splittings are possible: symmetric and antisymmetric parts, averages and deviations, large and small components, to mention three.

Supposing that the auxiliary equation

$$\frac{d\mathbf{U}(x)}{dx} = A(x)\mathbf{U}(x) \quad (6)$$

has already been solved subject to the initial condition $\mathbf{U}(x_0) = \mathbf{I}$, and that we intend to write $\mathbf{Z}(x) = \mathbf{U}(x)\mathbf{V}(x)$, we find that $\mathbf{V}(x)$ must solve the differential equation

$$\frac{d\mathbf{V}(x)}{dx} = \mathbf{U}(x)^{-1}B(x)\mathbf{U}(x) \mathbf{V}(x) \quad (7)$$

subject to the same initial condition as \mathbf{Z} .

3 Numerical integration with graphical presentation

However, to start from the beginning, consider the potential $\frac{1}{6}x^2$ with the differential equation

$$\frac{d\mathbf{Z}(x)}{dx} = \begin{pmatrix} 0 & m_0 + \frac{1}{2}x^2 - E \\ m_0 - \frac{1}{2}x^2 + E & 0 \end{pmatrix} \mathbf{Z}(x). \quad (8)$$

whose solution can be constructed numerically, at least.

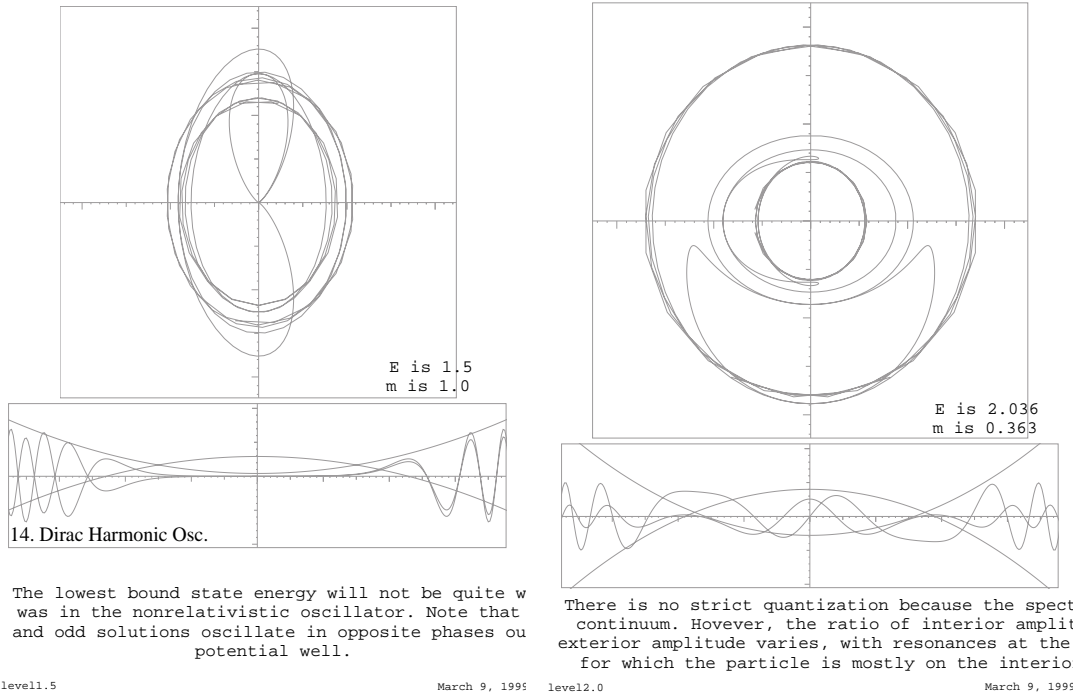


Figure 1: solutions and phase plane plots at two energies for the Dirac harmonic oscillator.

Figure 1 shows both the phase plane solution and the wavefunction graphed as a function of the independent variable. This is done for two different values of the energy, with a mass on the order of 1.0 in the units to which the equation is normalized (which is about 1% of the mass of an electron in the real world).

Both graphs tend to be fairly cluttered, especially when several options are activated simultaneously. The first thing to do is to locate the classically forbidden region, where the total energy is less than the potential with the mass added, yet greater than the potential with the mass subtracted. The result is a coefficient matrix with equal signs on the two sides of the diagonal resulting in hyperbolic motion. Or in other words, the wave function varies exponentially in this region, either growing or diminishing. In the phase plane, the trajectory will either run outwards towards an asymptote or inwards toward the origin in a complementary direction.

The classically allowed region, in which the coefficient is sign antisymmetric and the solution elliptical rather than hyperbolic, is either where a positive total energy lies above the mass shell or a negative total energy lies below it. In these regions the solution point in the phase plane will rotate around the origin with a velocity corresponding to the amount of kinetic energy available.

In combination, one will see two spirals separated in radius by an amount corresponding to the forbidden region.

The graphs of the individual components follows the same behavior, oscillating in accessible regions and changing overall amplitude in the forbidden regions. The feature which distinguishes resonances from other solutions is that the ratio of inside amplitude to outside amplitude is greater than 1 and as large as possible within its local region. Conversely, an antiresonance is an energy value for which the ratio is reversed, and the amplitude within the well is minimal. The distinction between interior and exterior is one of what the potential is doing at infinity, compared to what it is like near the origin.

4 Zero mass and its subsequent enhancement

Taking up the options offered by Equations 3 and 4 occasioned by setting the particle's mass to zero, the solution matrix for the massless Dirac harmonic oscillator would use the angle

$$\begin{aligned}\varphi(x, 0) &= \int_{x_0}^x \left(\frac{1}{2}t^2 - E \right) dt \\ &= \left[\frac{1}{6}t^3 - Et \right]_0^x \\ &= \frac{1}{6}x^3 - Ex\end{aligned}\tag{9}$$

to give the solution

$$\mathbf{Z}(x) = \begin{pmatrix} \cos(\frac{1}{6}x^3 - Ex) & -\sin(\frac{1}{6}x^3 - Ex) \\ \sin(\frac{1}{6}x^3 - Ex) & \cos(\frac{1}{6}x^3 - Ex) \end{pmatrix} \mathbf{Z}(0),\tag{10}$$

which is a pure rotation in the phase plane of rapidly increasing angular velocity. As a rotation, it will always describe solutions of constant amplitude.

When it comes time to include the mass in the solution, we need to work out the supplementary coefficient for \mathbf{V} which is $m_0\mathbf{j}$ transformed by \mathbf{U} . Here \mathbf{j} is the symmetric off-diagonal quaternion. Since it anticommutes with the *antisymmetric* off-diagonal \mathbf{i} and given that $\mathbf{U} = \exp(\varphi\mathbf{i})$ we get altogether

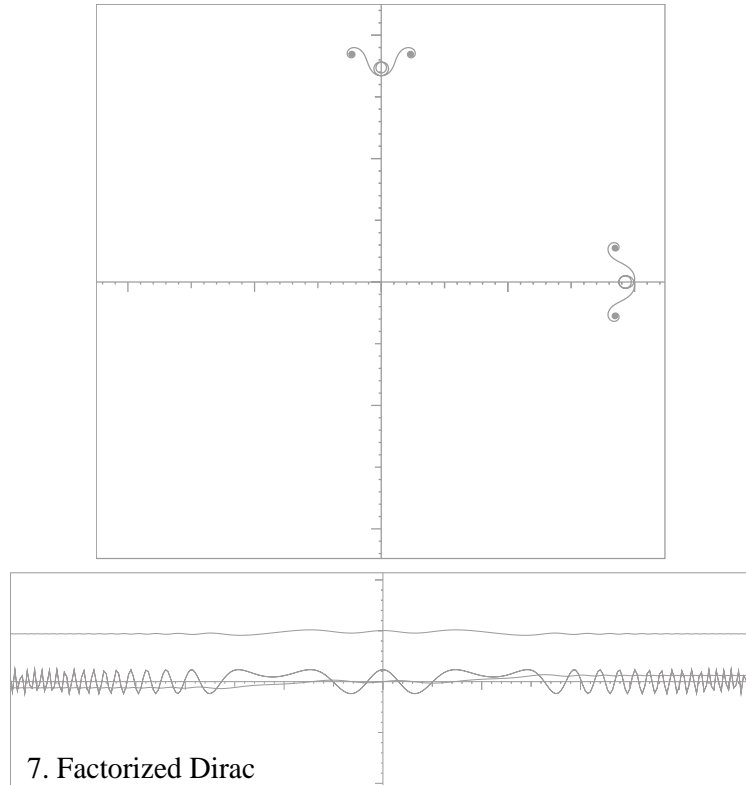
$$\mathbf{j} e^{\varphi\mathbf{i}} = e^{-\varphi\mathbf{i}} \mathbf{j},\tag{11}$$

and accordingly

$$\mathbf{U}^{-1}m_0\mathbf{j}\mathbf{U} = m_0 \begin{pmatrix} -\sin(\frac{1}{3}x^3 - 2Ex) & \cos(\frac{1}{3}x^3 - 2Ex) \\ \cos(\frac{1}{3}x^3 - 2Ex) & \sin(\frac{1}{3}x^3 - 2Ex) \end{pmatrix} \mathbf{Z}(0),\tag{12}$$

which is a rotating mirror. When it rotates rapidly it will confuse the solution point, leaving it nearly constant. But when rotating slowly, as it does near the classical turning points, it can provoke considerable change in a solution matrix, as it also does when it is counterrotating.

When the matrices \mathbf{U} and \mathbf{V} are combined to get the complete solution $\mathbf{Z} = \mathbf{UV}$ it is helpful to observe that one interpretation of a matrix product is that the second factor forms linear combinations of the columns of the first factor. Doing so, the solutions inherent in the matrix \mathbf{V} are just rewritten in the basis defined by \mathbf{U} , but otherwise interpreted as any other solution would be.



When the coefficient matrix of a differential equation is a sum of two terms, the overall solution matrix can be written as a product of one solution matrix by a constant matrix of the other. Here the electron mass is the additive term, giving solutions relative to a massless particle.

factor2.

March 9, 1995

Figure 2: The coefficient matrix in the one dimensional Dirac equation can be split into a mass term and an energy term. Solving the energy first allows the mass to be included later on.

Figure 2 shows how little the mass eventually matters in comparison to the energy for a consistently increasing potential such as the parabolic potential well of the harmonic oscillator. On the other hand, near the classical turning points and through the forbidden zone, there are appreciable discrepancies which are more clearly evident in the diagrams of the factored

potential than they were in their original form.

In principle, there is no reason why the factorization implementing the law of exponents for matrices should not be performed in the opposite order, regarding the mass term as fundamental. It would simply generate hyperbolic functions, with respect to which the energy terms would drive a rotating mirror which could be expected to raise and lower amplitudes passing from resonances to antiresonances.

After all, the final result is independent of the order of factorization.

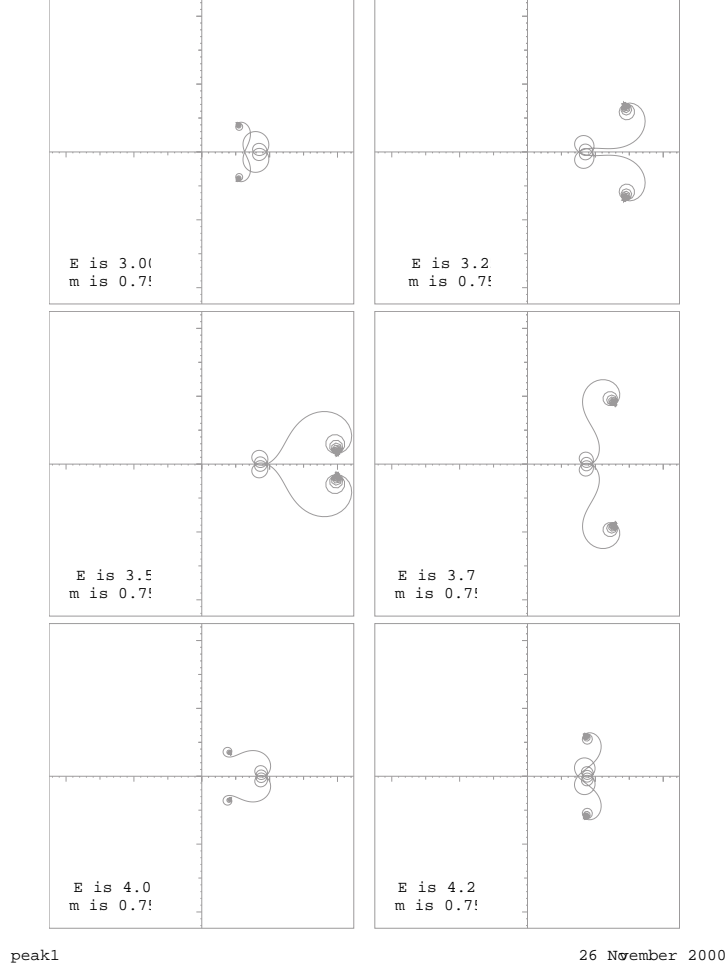


Figure 3: The auxiliary factor shown in the phase plane for a series of energies between a resonance and an antiresonance. The tight centers of the spirals represent asymptotic values at infinity, where the mass has little influence on the potential. Due to the symmetry of the potential, the phase diagram at resonance and antiresonance is also symmetric.

In Figure 3 a series of six phase planes is shown, straddling the interval of energies between one resonance and the next. The point to be observed is the changing relationship between the amplitude of the interior wave function and the amplitude of the exterior wave function.

The phase planes are shown separately to make the progression of ratios clearly evident. But then, for purposes of comparison, all six planes have been superimposed in Figure 4, where the magnitude of the variation is easier to discern.

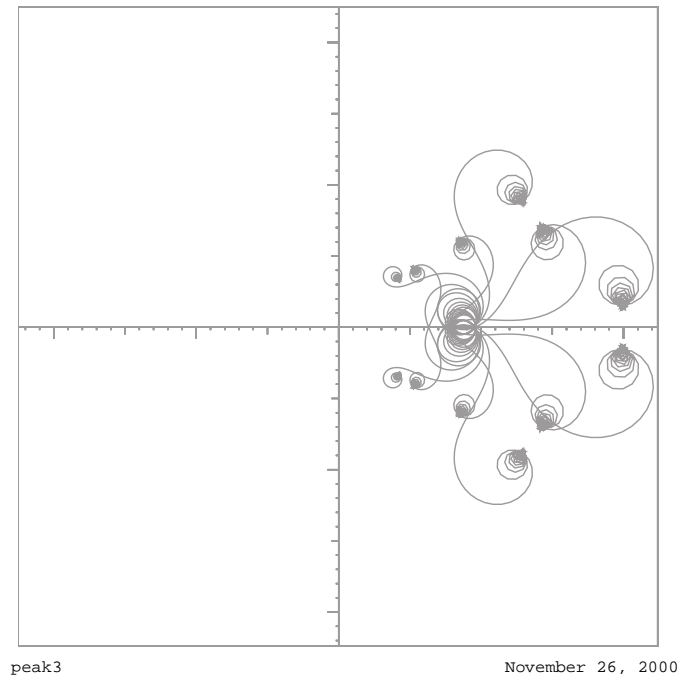


Figure 4: For ready comparison, all the trajectories comprising Figure 3 have been superposed, to get a design which would do many a peacock proud.

5 The Weyl-Titchmarsh m -function

Once that it has been established that there are resonances, it becomes a question of how to treat them analytically. Strictly speaking, this should be done for complex energies even though the differential equation is real, because there is a criterion for boundedness and unboundedness and a way of working with square-integrable solutions.

In practice, most of the information can be gotten from an examination of the real solutions, the only substantive question being the one of evaluating the amplitude at infinity for continuum wave functions. Symmetry can be a considerable asset, when it is present, because the solutions will fall into irreducible representations of the symmetry group. Thus for a harmonic oscillator well centered at the origin, solutions can be either even or odd.

If the prolongation of a symmetric solution has components $A \cos \theta, B \sin \theta$, the traditional substitution

$$R = \sqrt{A^2 + B^2} \tag{13}$$

$$\delta = \arctan(B/A) \tag{14}$$

will rewrite the components in terms of $R \cos \delta$ and $R \sin \delta$, so R would be the sought amplitude.

More complete details of this procedure can be found in the differential equation textbook of Coddington and Levinson [9], which is one of the very few which take up the topic of spectral densities and spectral matrices. Generalities, including a fair part of the treatment of the Dirac harmonic oscillator which is repeated here, can be found in McIntosh's contribution to Loebel's second volume on group theory [7]. The explicit reduction of the boundary value problem into three levels of symmetry, including the spectral distribution matrix, can be found in his contribution to Löwdin's Festschrift [8].

Figure 5 shows a hidden surface plot of the reciprocal of R around one of the resonances of the Dirac harmonic oscillator. Actually, having used R to normalize the wave function, the quantity which is graphed is the probability amplitude, which, for the Dirac equation, is the sum of the squares of the two components of the wave function.

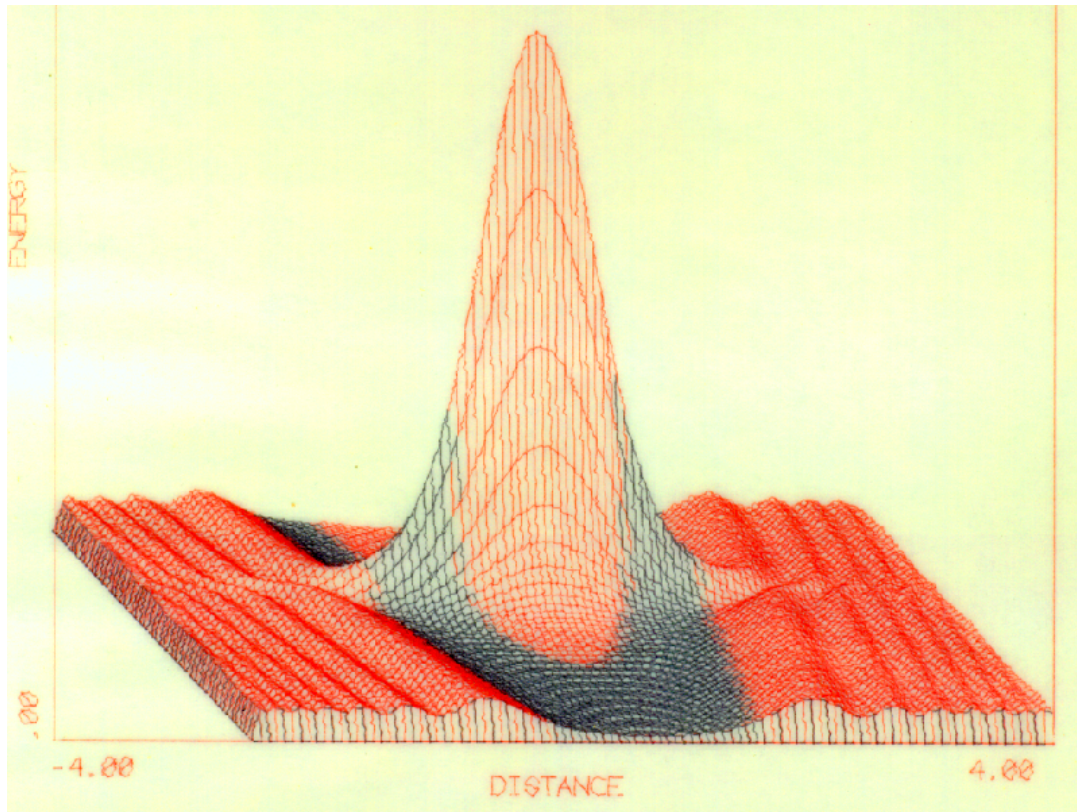


Figure 5: The region colored in black is the classically forbidden region, where the wave function is exponential.

This graph is one of many produced by the PDP-10 program <PL0T75>, this one exploiting the use of colored pens to color the resonance peak according to the location of the classically

forbidden region. This is the region in which the phase of the wave function at the classical turning point decides whether it will grow or shrink as it crosses the forbidden region, and emerging at the other classical turning point, fixes the amplitude of the wave function in the antiparticle region.

Since surface coloring can be used to exhibit whatsoever property of the wave function, Figure 6 is used to show the phase of the wave function rather than the square of its amplitude.

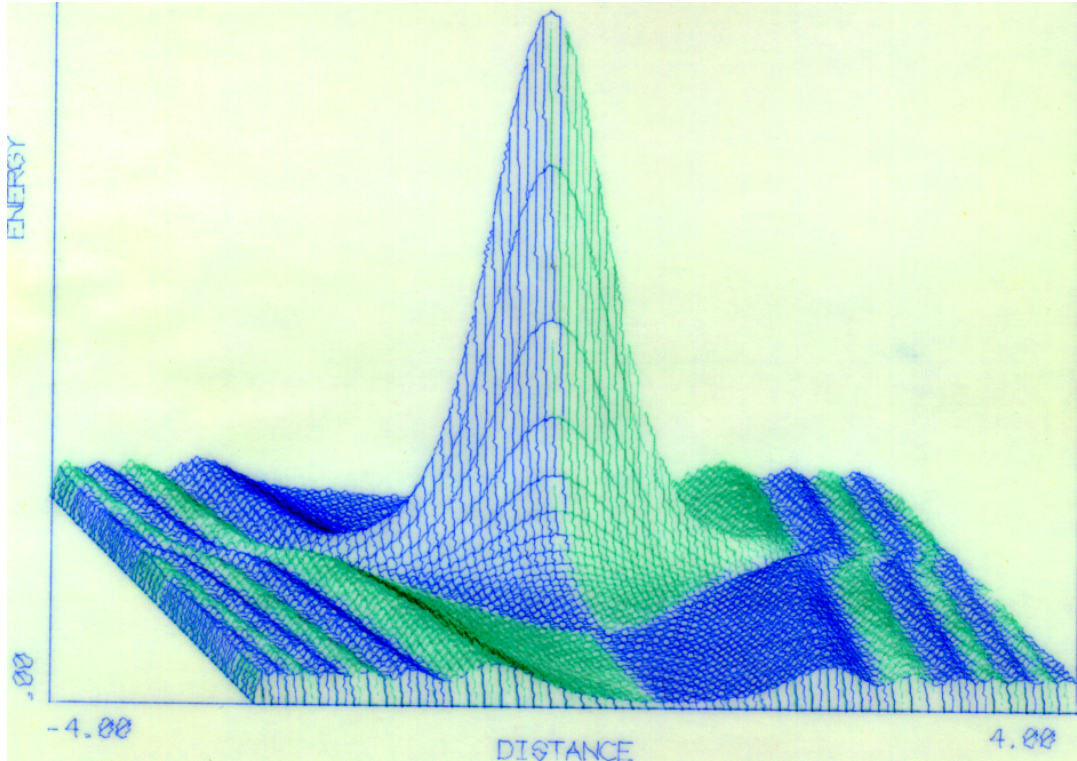


Figure 6: Although the surface represents probabilities, it is colored according to the phase of the wave function.

The object displayed in the figure is the resonance peak corresponding to what would be the ground state in the nonrelativistic or infinite-mass limit. It therefore resembles a cosine (more precisely, a gaussian) and is even. The quantity coloring the surface is evidently the situation of the solution vector in the left or right half of the phase plane so that each undulation of the surface carries the point halfway around the origin.

The most instructive feature of all these graphs is the phase change of the wave function with increasing energy on passing a resonance peak. Crests in the wave surface follow the parabolic potential at a respectful distance, but a new crest is born at each resonance and pushes the others out, further away from the forbidden region. In other words, an 180° phase

shift accompanies each resonance crossing.

Another detail to be noticed is the rapidity with which the undulations die down to a fairly constant height, which of course is their asymptotic value. But they wiggle faster and faster, this being due to the x^3 factor dominating their phase.

In Figure 7 the same surface is repeated once again, this time colored in bands of constant energy increment. There is no reason why a checkerboard could not have been built up, by switching colors following a constant increment in x , but such things have to be planned before making the graph, not afterwards.

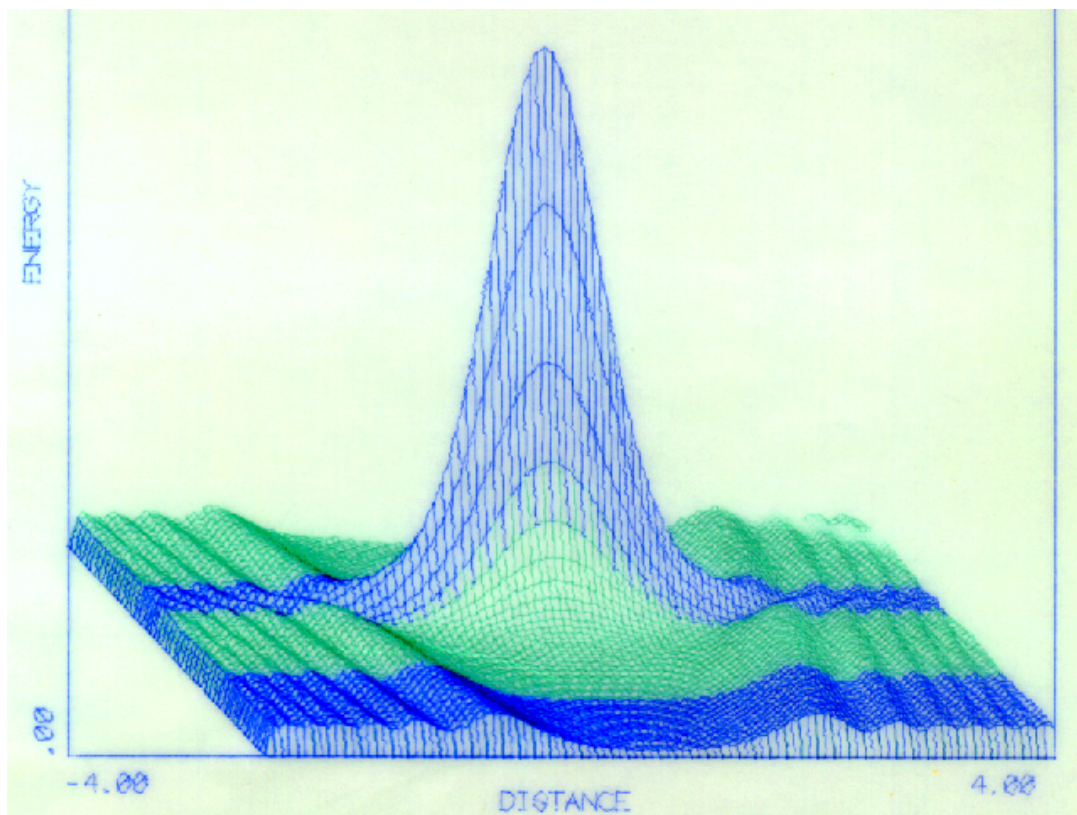


Figure 7: Although the surface represents probabilities, it is colored according the value of the energy, in strips of unit increment, thereby allowing a quick estimate of the eigenvalues.

Since one band nicely straddles the peak, the flow of crests in the antiparticle region still receives its nudge from the resonance, with its impact on the artistic value of the picture.

Although they are not always planned, artifacts of the drawing program frequently induce elements of texture into the image they are producing. Sometimes the result is only a pleasing appearance, something which turns out to be rather subjective. Other times, the moirés produced reveal the flatness of the image, or abrupt changes such as edges, depressions, or protrusions. If the moiré is very regular, that is evidence that the image is quite smooth.

Useful as perspective drawings with hidden line suppression are for visualizing phenomena, they are still complementary to contour maps, such as the one shown in Figure 8, which encompasses three successive resonances, starting with the one depicted in the previous Figures. It was an experiment, using a thick pointed pen with colored ink to try to fill in an area rather than simply mark out lines.

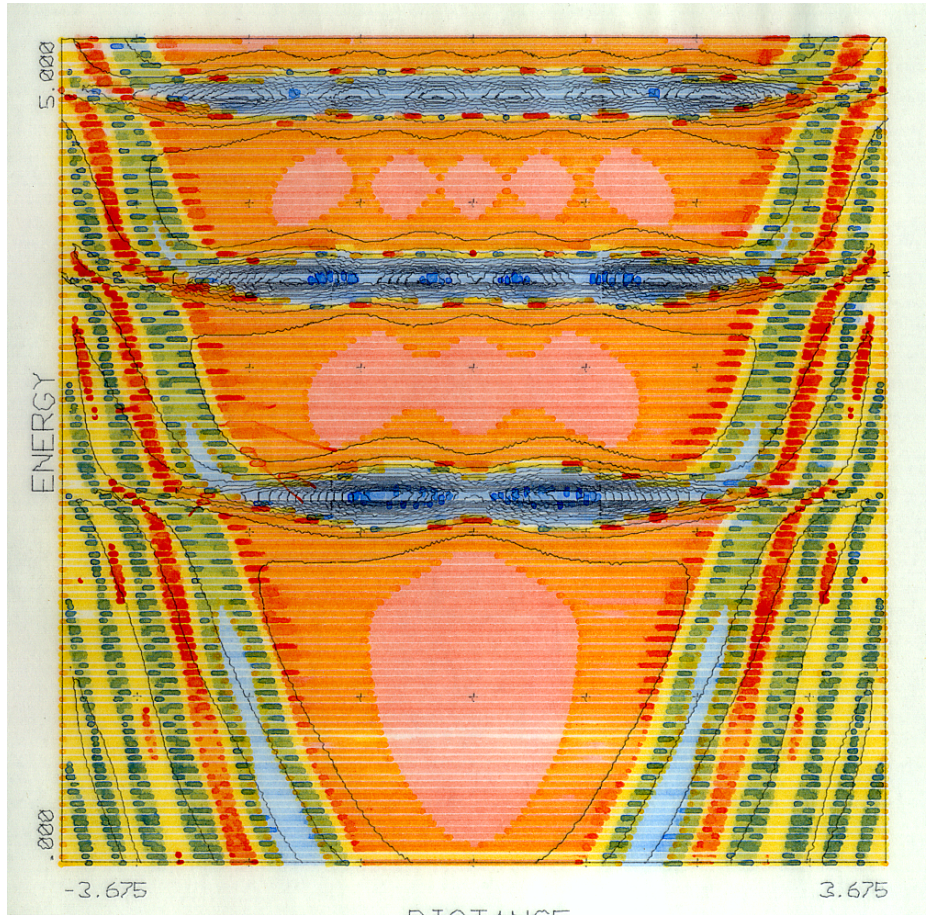


Figure 8: Contour map of the probability density for the odd solutions of the Dirac harmonic oscillator equation. There would be a corresponding map for the odd solution. Since the potential is symmetric, we know that parity determines the eigenfunctions, without having to diagonalize the spectral density matrix.

Because of the parity of the initial condition, contour maps such as these show either the even resonances or the odd resonances. The vertical viewpoint shows the flow of crests around resonances quite clearly. Notice that the antiresonances have just as much interior structure as the resonances; in fact there is a fairly reciprocal relationship for amplitudes.

In some versions of this drawing, the classically forbidden region has been overlaid, showing

quite clearly that all the crest shifting goes one in and at the margins of that region.

Returning to perspective drawings, Figure 9 encompasses a broader range of peaks, more in keeping with the range of the contour map.

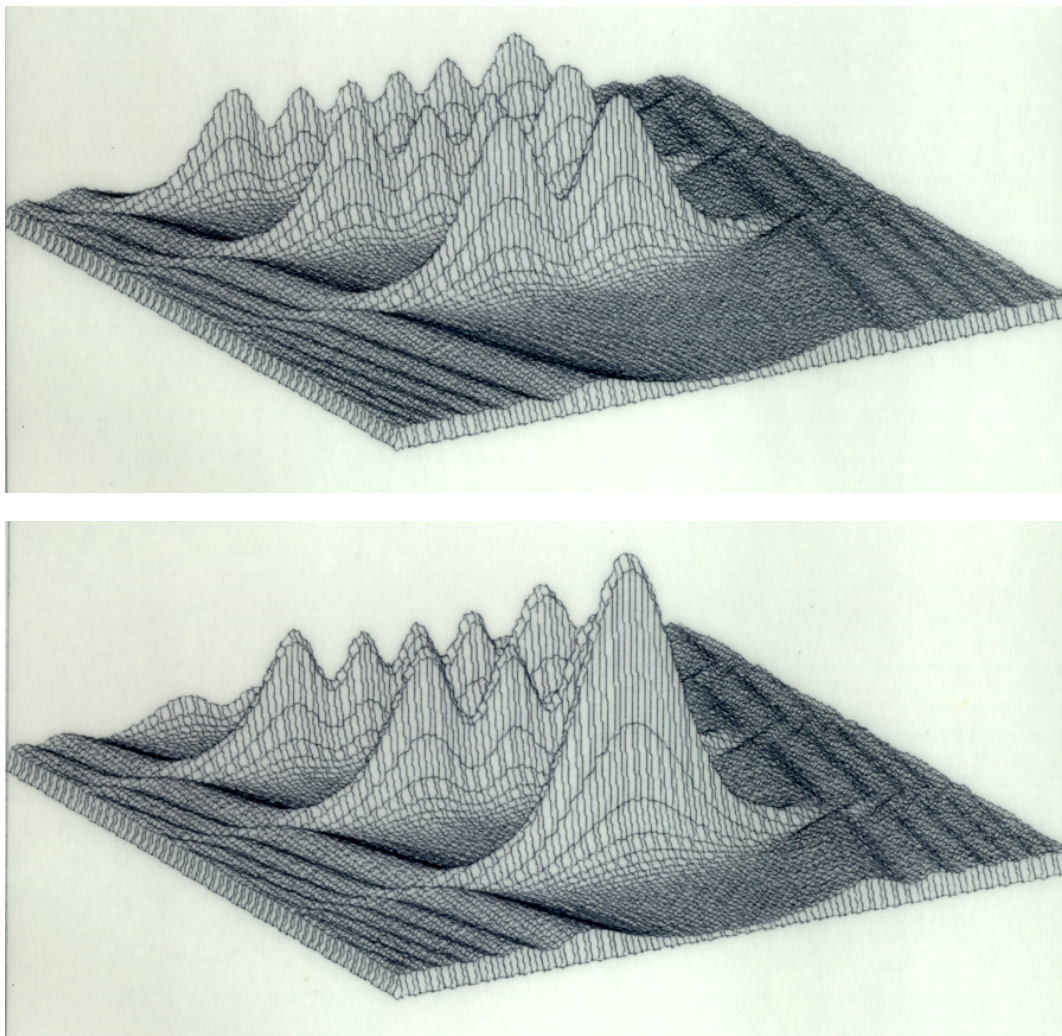


Figure 9: Probability amplitudes for even (lower image) and odd (upper image) solutions.

Much planning can, or at least should, go into preparing drawings of functions. For example, the angle of view and relative compactness of Figure 9 allows further insight into the crest arrangement of the Dirac harmonic oscillator. Some conclusions can be drawn about the relative amplitudes of the different resonances, but it should not be supposed that they are normalized. On the contrary, their defining characteristic is unit amplitude at infinity. Under those circumstances none of the solutions can be normalized, and the most that can be expected is that they will play their part in the definition of the spectral density function

via the Stieltjes integral.

6 Dependence of spectral density on mass

The weight function for the Stieltjes integral definition of the spectral density is substantially that it is the value at the origin of a wave function of unit amplitude at infinity. In order to better grasp this concept, Figure 10 repeats the resonance graph of Figure 5 (and those following it), having been truncated at the origin with a perspective showing the starting amplitude in clear outline.

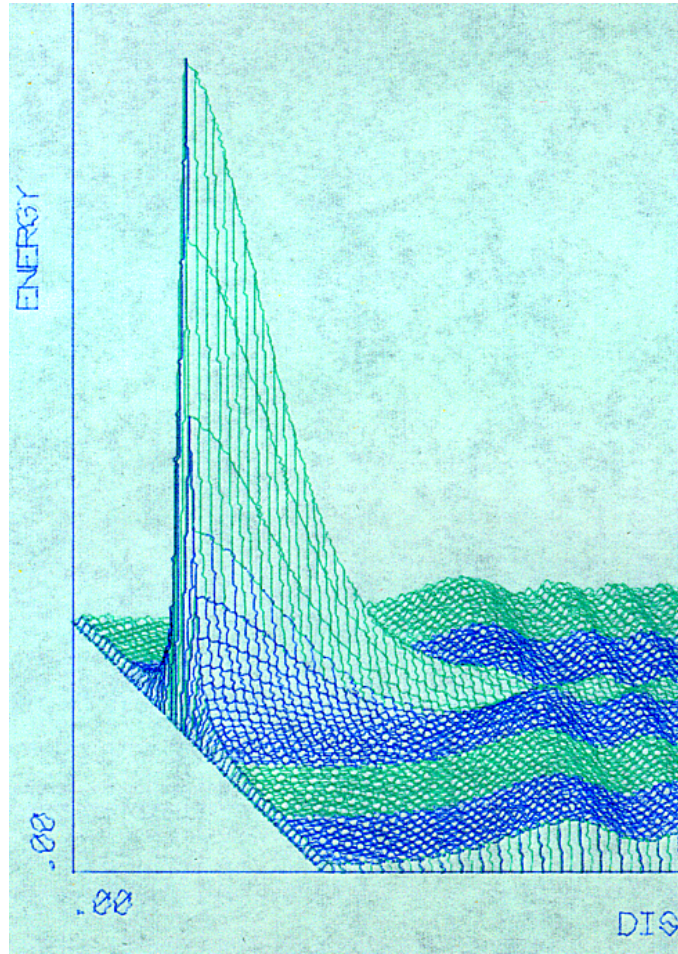


Figure 10: The spectral density function is the absolute value at the origin of the wave function normalized to absolute value 1 at infinity. The resonance has been sliced to show its behavior at the origin clearly.

Figure 11 exhibits another kind of graph which would be of interest, namely the result of

showing only the trace across the origin featured in Figure 10, but for varying masses. The result could run from zero mass, without any classically forbidden region at all, to a large enough mass that it would correspond to actual electrons in atoms. That would be the limit which interested Sewell [5] and Titchmarsh [6].

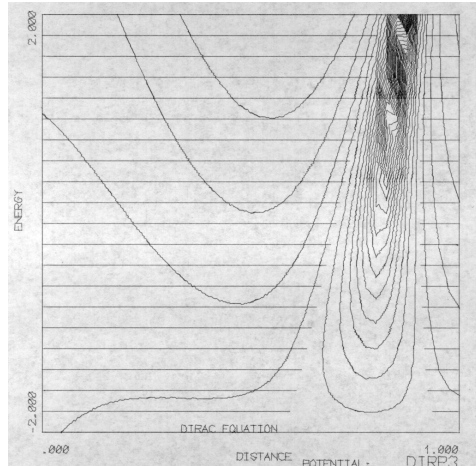
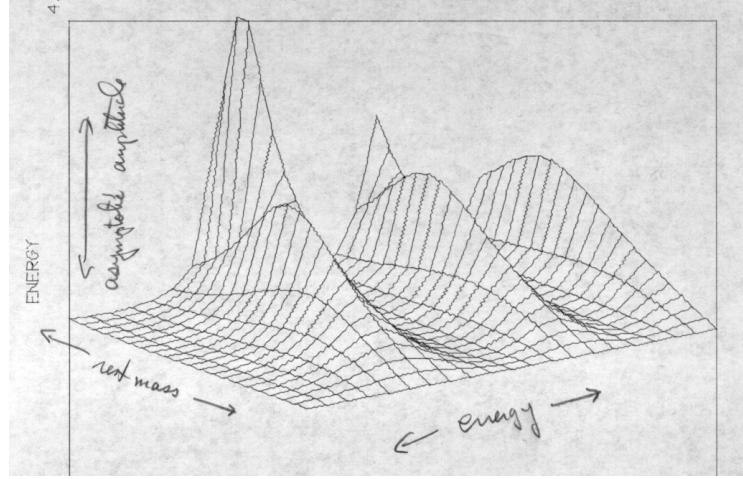


Figure 11: The spectral density function is the absolute value at the origin of the wave function normalized to absolute value 1 at infinity. The apparent discontinuity in the second peak of the top figure is due to the egg-crate effect, and is not a break.

The peaks in these functions, especially in the limit of large masses, suggest the interpretation of the Dirac harmonic oscillator in terms of complex energies and associated eigenfunctions.

References

- [1] P. A. M. Dirac, "The quantum theory of the electron," *Proceedings of the Royal Society of London*, **A117** 610-624 (1928).
- [2] H. Weyl, "Über gewöhnliche Differentialgleichungen mit Singularitäten und die zugehörige Entwicklungen willkürlicher Funktionen," *Mathematische Annalen* **68** 220-269 (1910).
- [3] K. Nikolsky, "Das Ozillatorproblem nach der Diracschen Theorie," *Zeitschrift für Physik* **62** 677-681 (1930).
- [4] I. Postepska, "Harmonische Ozillator nach der Diracschen Wellengleichung." *Acta Physica Polonica* **4** 269-280 (1935).
- [5] G. L. Sewell, "An approximate relation between the energy levels of a particle in a field of a given potential energy, calculated on the relativistic and non-relativistic theories," *Proceedings of the Cambridge Philosophical Society* **45**. 631-637 (1949).
- [6] E. C. Titchmarsh, "On the relation between the eigenvalues in relativistic and non-relativistic quantum mechanics," *Proceedings of the Royal Society, Series A* **266**, 33-46 (1962); *Quarterly Journal of Mathematics* **15**, 193-207 (1964).
- [7] Harold V. McIntosh, "Quantization as an Eigenvalue Problem," In *Group Theory and Its Applications*, Vol. 3, (Ernest M. Loebl Editor), Academic Press, New York (1975), pp. 333-368.
- [8] Harold V. McIntosh, "Quantization and Green's Function for Systems of Linear Ordinary Differential Equations," In *Quantum Science: Methods and Structure*, Edited by J. L. Calais, O. Goscinsky, J. Linderberg and Y. Ohn, Plenum Press, New York (1976) pp. 227-294.
- [9] Earl A. Coddington and Norman Levinson, *Theory of Ordinary Differential Equations*, McGraw-Hill Book Company, Inc., New York, 1955.

January 11, 2001